

Revisiting default mode network function in major depression: evidence for disrupted subsystem connectivity

Fabio Sambataro^{1,*}, Nadine Wolf², Maria Pennuto³, Nenad Vasic⁴, Robert Christian Wolf^{5,*}

¹Brain Center for Motor and Social Cognition, Istituto Italiano di Tecnologia@UniPR, Parma, Italy; ²Department of Addictive Behavior and Addiction Medicine, Central Institute of Mental Health, Mannheim, Germany; ³Neuroscience and Brain Technology, Istituto Italiano di Tecnologia, Genova, Italy; ⁴Department of Psychiatry and Psychotherapy III, University of Ulm, Ulm, Germany; ⁵Center of Psychosocial Medicine, Department of General Psychiatry, University of Heidelberg, Germany

Supporting Information

Participants. Fourteen patients were treated with psychotropic medications (see Tab. S1). None of the patients were receiving a stable regime of benzodiazepines at the time of the fMRI measurements.

Patient #	Drug treatment
1	Escitalopram 10 mg
2	Escitalopram 10 mg
3	Escitalopram 10 mg
4	Escitalopram 15 mg
5	Escitalopram 20 mg, Agomelatine 25 mg
6	Fluoxetine 30 mg, Agomelatine 50 mg
7	Paroxetine 20 mg, Mirtazapine 15 mg
8	Sertraline 200 mg, Pregabalin 600 mg
9	Venlafaxine 75 mg
10	Venlafaxine 75 mg, Mirtazapine 30 mg
11	Duloxetine 90 mg, Mirtazapine 45 mg
12	Duloxetine 30 mg, Agomelatine 25 mg
13	Mirtazapine 15 mg
14	Bupropion 300 mg

Tab. S.1. Individual drug treatment in patients with MDD at the time of the scan

Clinical and demographic features of patients with and without treatment did not differ (Mann Whitney U test, all p's>0.2, see Tab. S.2).

Feature	Drug-free MDD	MDD	U	exact p
Age (M±SD, years)	35.33±11.5	39.07±8.93	29.5	0.311868
Education (M±SD, years)	12.67±0.52	13.21±2.01	41	0.967957
Edinburgh Handedness Inventory (M±SD)	86.67±21.6	88.64±16.73	42	1
Beck Depression Inventory (M±SD)	32.17±8.68	26.64±8.76	27	0.239112
Hamilton Rating Scale for Depression (M±SD)	23.33±4.89	21±3.72	31	0.397007

Tab. S.2. Demographic and clinical features of drug-free and treated patients with MDD. U, Mann Whitney U statistics of the differences between the two groups; p, p-value of these differences

Imaging Analysis. After discarding the first 8 volumes of the time series to account for MRI equilibration effects, all functional volumes were realigned to the mean volume using Fourier interpolation. To exclude that the effects of diagnosis were biased by motion extent differences, we computed average Euclidean distance from the first scan for each subject and compared them across diagnostic groups. We did not find any difference for this parameter (MDD, 0.13 ± 0.06 mm; HC, 0.14 ± 0.09 mm; $p=0.52$). Before entering the ICA, realigned data were skull-stripped, intensity normalized, smoothed with a 6-mm FWHM isotropic 3D Gaussian kernel, linearly detrended and converted to Z-scores. Before entering LFF analysis, realigned data were temporally despiked with a hyperbolic tangent squash, linearly detrended, spatially smoothed with a 6-mm FWHM isotropic kernel and grand-mean scaled.

Registration. Each individual's high-resolution structural image was registered to the Montreal Neurological Institute 152-brain (MNI-152) template using a linear affine transformation with 12 degrees of freedom. This transformation was then applied to each individual's data with 3-mm isotropic voxel size before the performing the ICA and at the end of the LFF analysis, respectively.

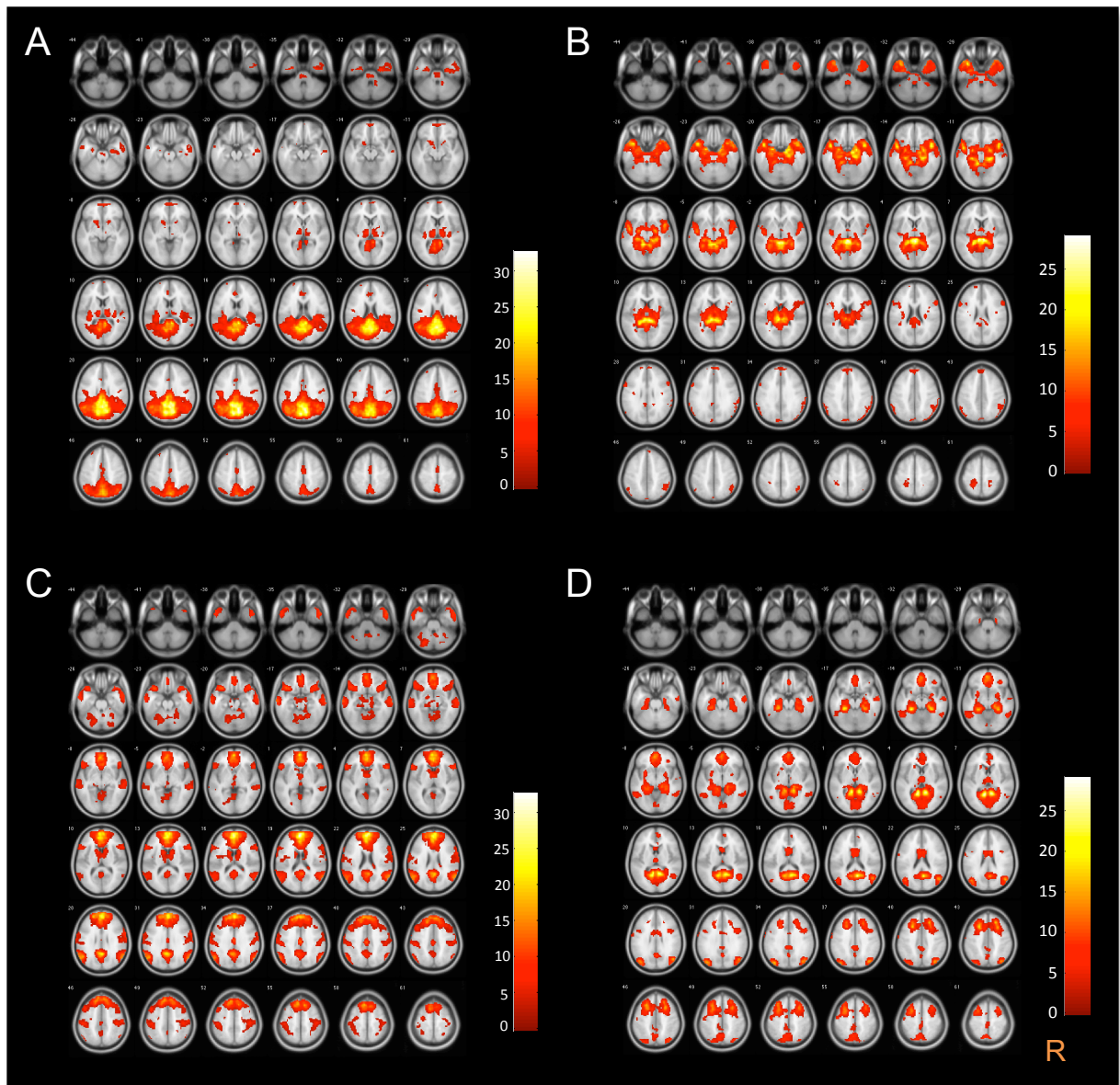


Fig. S.1. The DMN subsystems. The DMN entailed four distinct subsystems: the posterior DMN (A), the ventral DMN (B), the anterior DMN (C) and the core DMN across all subjects. Coronal projections of the T-maps of DMN subsystem connectivity are thresholded with a voxel-wise $p=0.001$ and corrected for multiple comparisons at the level of cluster ($p=0.05$) and overlaid on the Montreal Neurological Institute brain template. Color bar indicates T-scores. R, right.

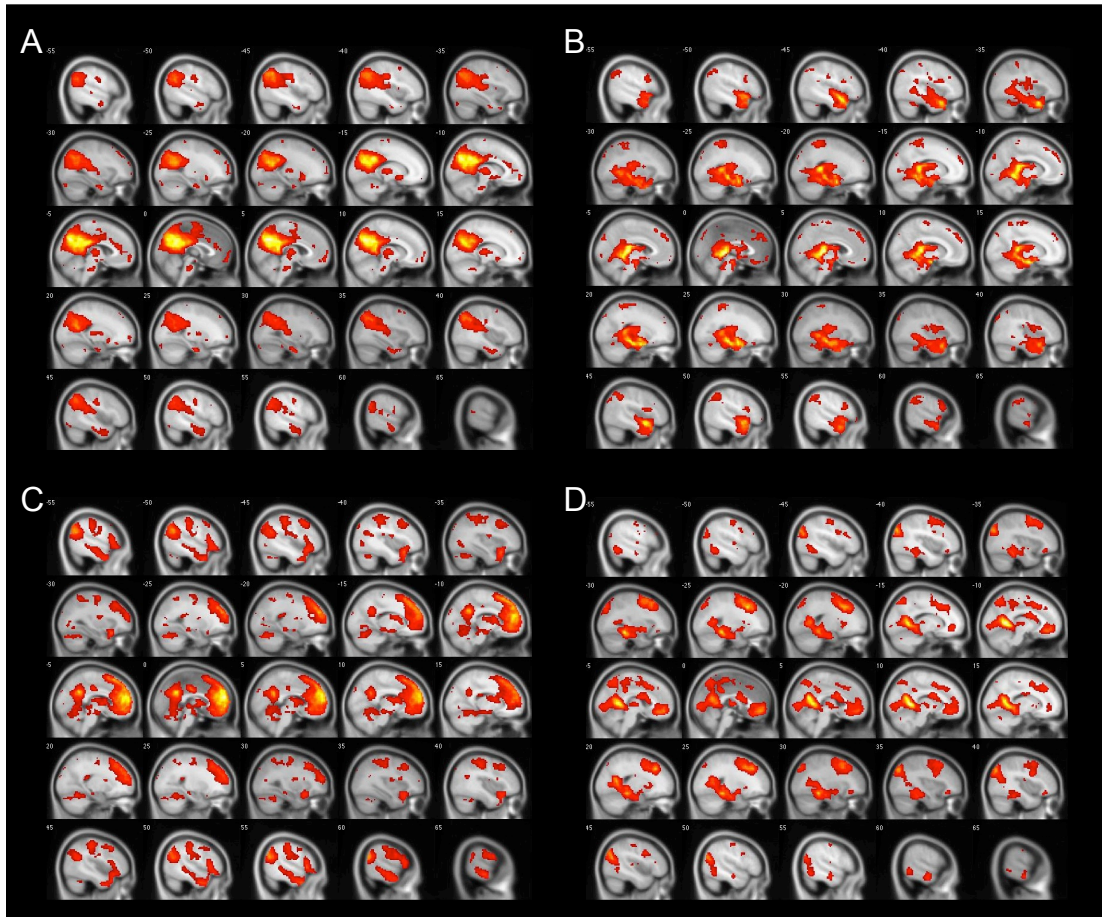


Fig. S.2. Spatial extent of the DMN subsystems. The posterior DMN (A), the ventral DMN (B), the anterior DMN (C) and the core DMN across all subjects are depicted at a liberal threshold. Sagittal projections of the T-maps of DMN subsystem connectivity are thresholded with a voxel-wise $p=0.005$ uncorrected and overlaid on the Montreal Neurological Institute brain template.

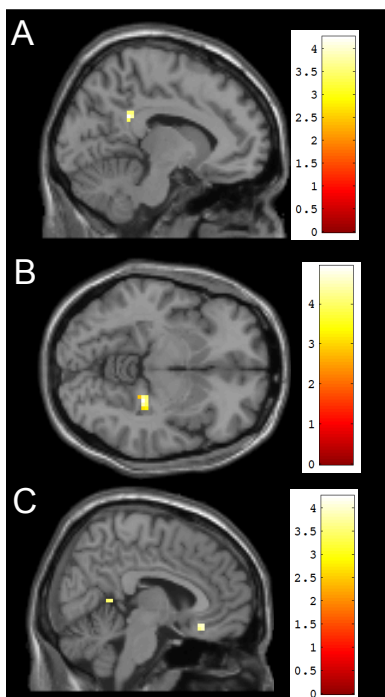


Figure S.3. Effect of diagnosis on functional connectivity within DMN subsystems after covarying out the effects of age. Patients with MDD had increased connectivity strength in posterior cingulate (A) within the posterior DMN, in right hippocampus (B) within ventral DMN, and subgenual and retrosplenial posterior cingulate (C) within the core DMN relative to healthy controls. Sagittal projections of the T-maps of DMN connectivity differences are thresholded with a voxel-wise $p=0.001$ and corrected for multiple comparisons at the level of cluster and overlaid on the MNI brain template. Color bar indicates T-scores.

Feature	Drug-free MDD (6)	HC (20)	U	exact p
Demographic and clinical variables				
Age (M±SD, years)	35.33±11.5	33.55±11.03	54.5	0.744473
Education (M±SD, years)	12.67±0.52	13.7±1.92	37	0.17559
Edinburgh Handedness Inventory (M±SD)	86.67±21.6	85.05±15.35	45	0.387456
Beck Depression Inventory (M±SD)	32.17±8.68	1.75±2.49	0	0.000009
Hamilton Rating Scale for Depression (M±SD)	23.33±4.89	0.9±1.52	0	0.000009
Imaging measures				
fALFF-pgCC (M±SD, a.u.)	1.49±0.53	0.6±0.55	14	0.003371
<i>posterior DMN</i>				
- PCC (M±SD, a.u.)	0.49±0.11	0.37±0.06	15	0.004326
<i>ventral DMN</i>				
- Hippocampus (M±SD, a.u.)	0.28±0.04	0.21±0.07	23	0.023298
<i>anterior DMN</i>				
- sgCC (M±SD, a.u.)	0.18±0.06	0.07±0.11	23	0.023298
- right Temporoparietal cortex (M±SD, a.u.)	0.33±0.11	0.09±0.11	6	0.000261
- retrosplenial cingulate (M±SD, a.u.)	0.56±0.09	0.4±0.09	13	0.002589
Granger causality				
- anterior DMN->ventral DMN (M±SD, a.u.)	0.22±0.27	0.02±0.04	27	0.045858

Tab. S.3. Demographic and clinical and imaging differences between drug-free patients with MDD and healthy controls (HC). U, Mann Whitney U-statistics of the differences between the two groups; p, p-value of these differences. M, mean; SD, Standard deviation; a.u., arbitrary units; fALFF, fractional amplitude of low frequency fluctuations; pgCC, perigenual cingulate cortex; sgCC, subgenual cortex. DMN subsystems connectivity is measured as the average of the voxel-wise IC loadings within a cluster showing the effect of diagnosis (Fig.1).

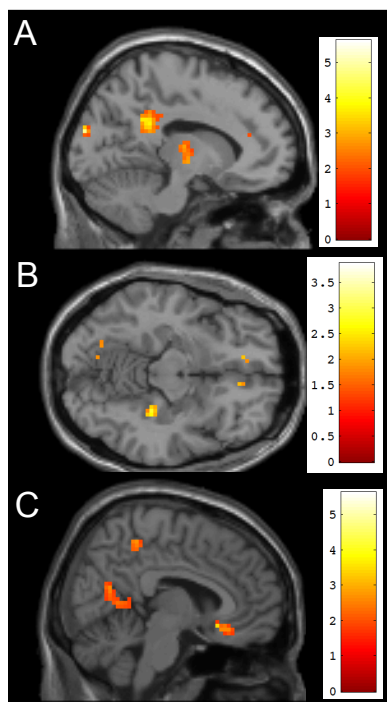


Figure S.4. Effect of diagnosis on functional connectivity within DMN subsystems in drug-free patients (6). Patients with MDD had increased connectivity strength in posterior cingulate (A) within the posterior DMN, in right hippocampus (B) within ventral DMN, and subgenual and retrosplenial posterior cingulate (C) within the core DMN relative to healthy controls. Sagittal projections of the T-maps of DMN connectivity differences are thresholded with a voxelwise $p=0.005$ and overlaid on the MNI brain template. Color bar indicates T-scores.

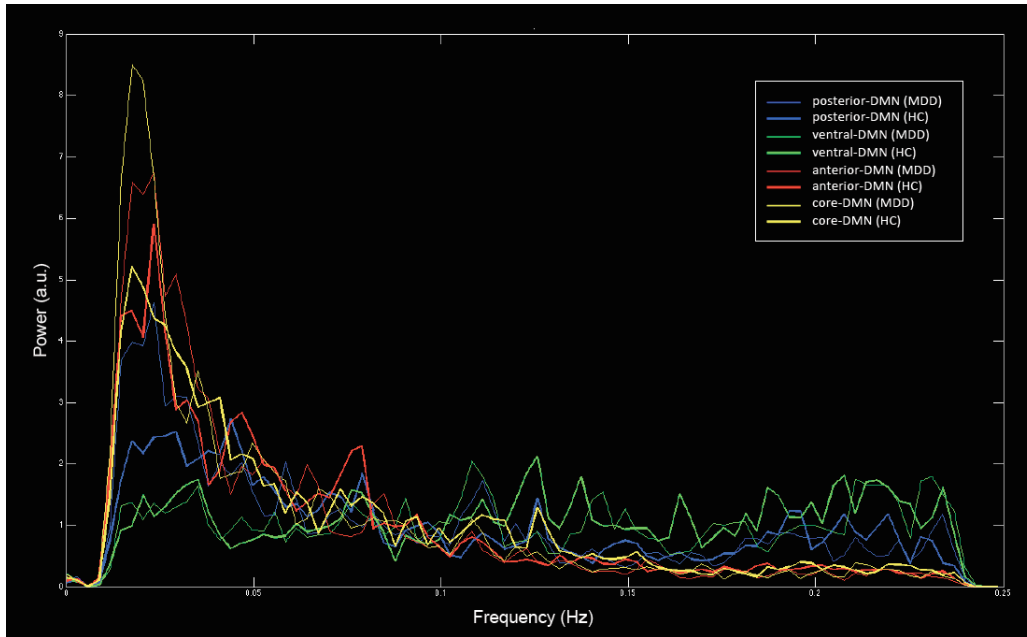


Fig. S.5. Effect of diagnosis on the power spectral analysis of the DMN subsystems. Colored lines show the power spectrum for posterior DMN (blue), ventral DMN (green), anterior DMN (red) and core DMN (yellow) for patients with MDD (thinner lines) and healthy controls (thicker lines). X-axis indicates power amplitude in arbitrary units, y-axis indicates frequency spectrum in Hertz (Hz).

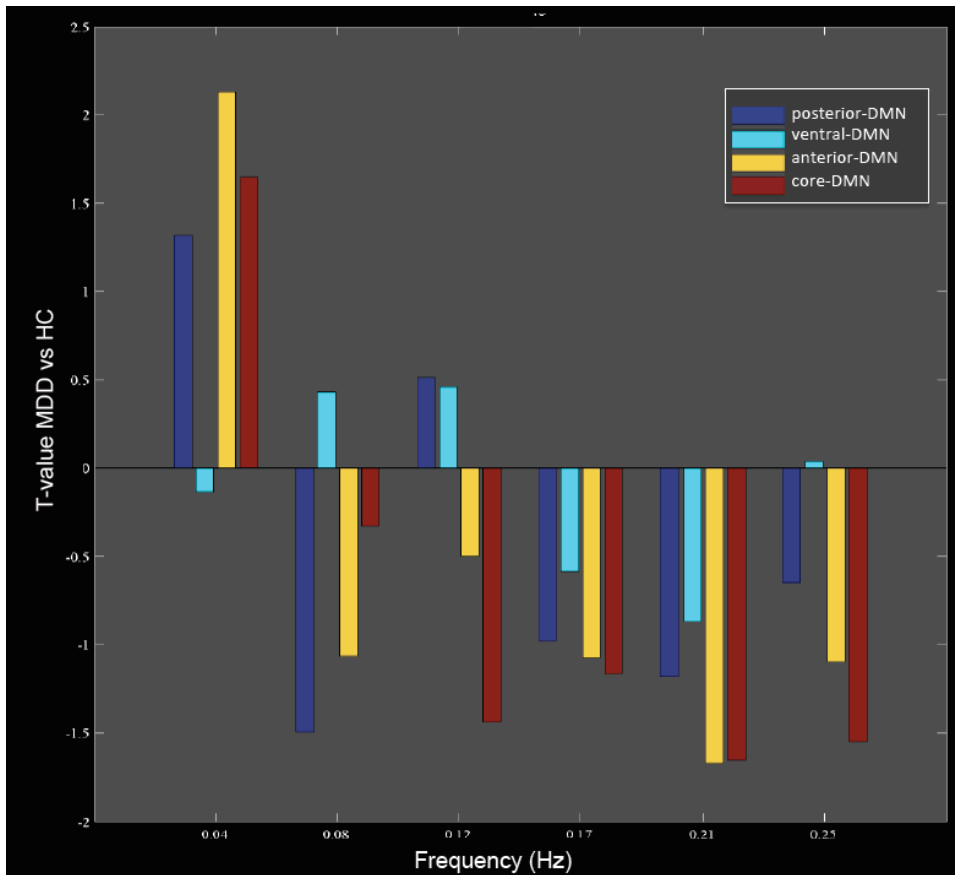


Fig. S.6. Effect of diagnosis on the frequency bins of the power spectral analysis of the DMN subsystems. X-axis indicates frequency bins, y-axis indicates the T-value for the MDD-HC comparison, grouped for each frequency bin and DMN subsystem. Histograms are colored by DMN subsystems: posterior DMN (blue), ventral DMN (cyan), anterior DMN (yellow) and core DMN (red)

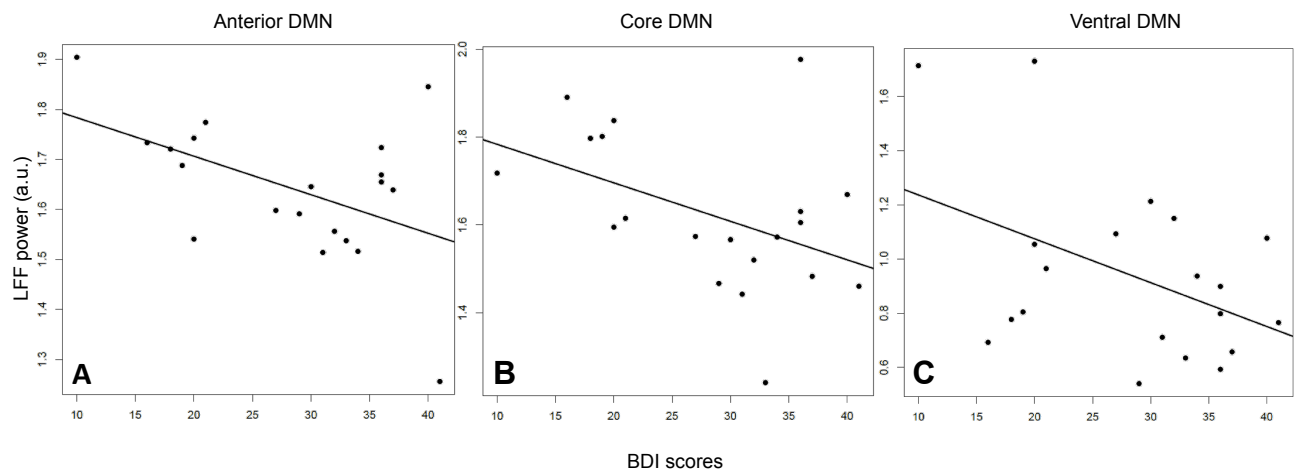


Figure S.7. Correlations between the low frequency fluctuations (LFFs) in core (A), ventral (B) and anterior DMN (C) subsystems and Beck Depression Inventory (BDI) scores. In patients with MDD, lower power of LFFs in DMN subsystems predicted greater MDD severity. X-axis indicates power spectrum in the 0.04 Hz bin, y-axis indicates BDI scores. Lines represent the best-fit lines.

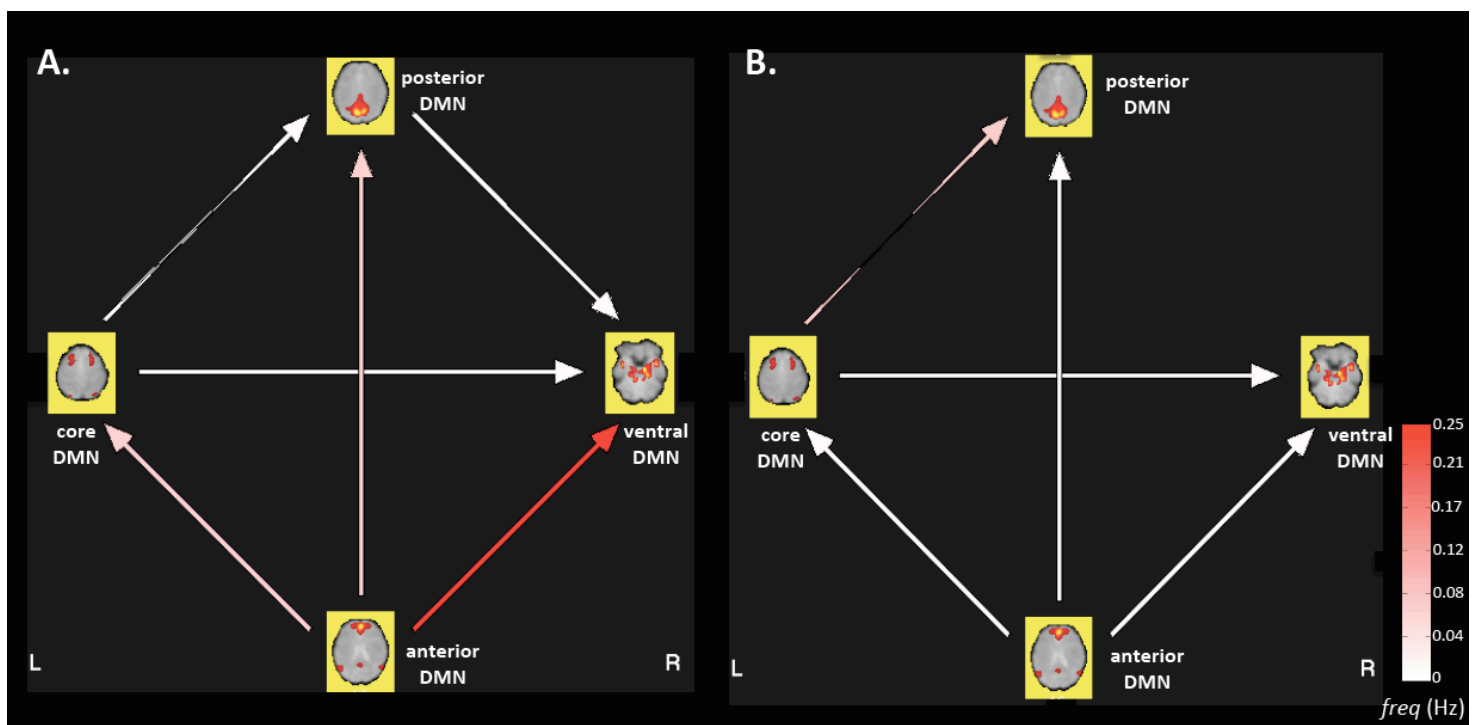


Fig. S.8. Functional network connectivity across DMN subsystems in patients (A) and healthy controls (B). Between-DMN subsystem connectivity is thresholded at $p < 0.05$ FDR. Arrows and color bar indicate the direction and the frequency of significant Granger causality tests, respectively. Color bar indicates frequency in Hertz (Hz)

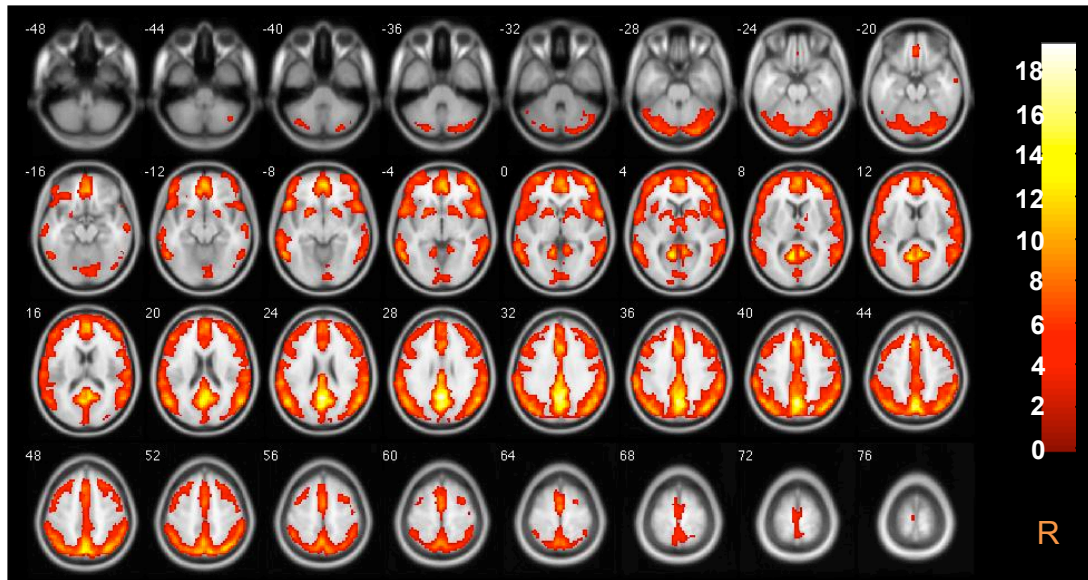


Fig. S.9. Fractional amplitude of the low frequency fluctuations (fALFF) in the entire group. Coronal projections of the T-maps of fALFF are thresholded with a voxel-wise $p=0.001$ and corrected for multiple comparisons at the level of cluster ($p=0.05$) and overlaid on the Montreal Neurological Institute brain template. Color bar indicates T-scores. Z-coordinates of coronal slice are indicated on the top left corner of each slice. R, right

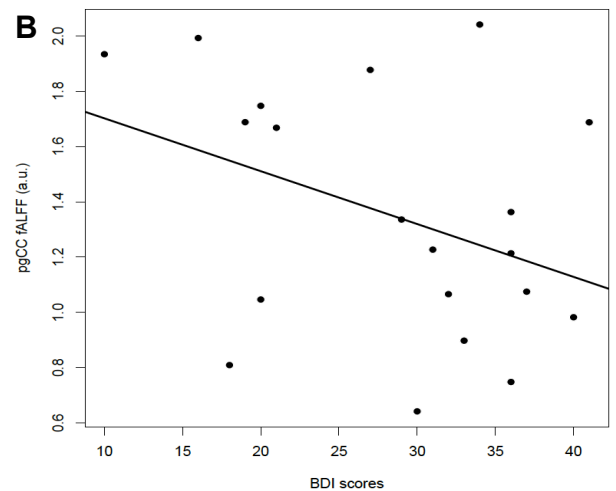


Figure S.10. Effect of diagnosis on the fractional amplitude of low frequency fluctuations (fALFF). Patients with MDD had increased connectivity strength in perigenual cingulate (A). fALFF correlated with depression severity measured using Beck Depression Inventory (BDI) scores (B, $r=-0.38$, $p=0.09$). The sagittal T-map of fALFF differences is thresholded with a voxel-wise $p=0.001$ and corrected for multiple comparisons at the level of cluster and overlaid on the Montreal Neurological Institute brain template. Color bar indicates T-scores. X-axis indicates BDI scores, y-axis indicates perigenual cingulate fALFF in arbitrary units.